

Parametric Sensitivity Analysis of Chromium (VI) Adsorption using *Theobroma Cacao* L Biomass via Process Simulation

Ángel Darío González-Delgado^a, Candelaria Tejada-Tovar^b, Angel Villabona-Ortiz^{b,*}

^aChemical Engineering Department, Nanomaterials and Computer-Aided Process Engineering Research Group (NIPAC), Universidad de Cartagena, Avenida del Consulado St. 30, Cartagena de Indias 130015, Colombia

^bChemical Engineering Department, Process Design and Biomass Utilization Research Group (IDAB), Universidad de Cartagena, Avenida del Consulado St. 30, Cartagena de Indias 130015, Colombia
avillabona@unicartagena.edu.co

Although several advances in heavy metal adsorption using biomass are being developed at lab scale, there is a lack of information regarding the behaviour of these emerging technologies from the technical point of view at higher scales, *Theobroma cacao* residues had shown a good performance towards Chromium (VI). Subsequently, this study was conducted to develop the parametric sensitivity analysis of Cr (VI) removal from aqueous solution onto an adsorbent based on cocoa husk, using Aspen Adsorption® V10 software based on data from batch experiments. A dynamic column performance was evaluated systematically while varying in three levels the feed flow (0.75, 1.5 and 3 mL/s), initial concentration (10, 30, 50 and 100 mg/L), bed height (30, 65 and 100 cm) and particle diameter (0.5, 1 and 2 mm) and their effect over the breakthrough curve. The simulated parameters showed great sensitivity towards bed height and inlet flows in the performance of the column by delaying or shorting the breakthrough time.

1. Introduction

Chromium is a pollutant that can be found in the effluents of various industries such as metallizing, tanneries, mining operations, electroplating industries, fertilizer, pesticide and battery industries (Dinh Thi, 2021). Chromium (VI) is a mutagenic contaminant and causes cancer of the lungs, nose, and sinuses; thus, the maximum concentration allowed according to the US-EPA is 0.05 mg/L (Ben Khalifa et al., 2019). It could pose a risk to living organisms even at low concentrations and received warnings, especially when the polluted water body is used as drinkable water for human existences (Manjuladevi et al., 2018). Although many treatment alternatives had been implemented to remove compounds of chromium, adsorption is still regarded as an efficient alternative based on its performance and cost (Gómez-Aguilar et al., 2019). Adsorption techniques have been used to remove certain classes of chemical pollutants from waste-water, such as metallic ions (Malise et al., 2020), demonstrated that various adsorbents of agricultural and agro-industrial origin due to their biodegradability, sustainability, low cost, renewability and rich surface with functional groups (Afroze and Sen, 2018); adsorbents such as peas (ul Haq et al., 2017), rice straw (Wu et al., 2016), lanzon (Lam et al., 2016), cocoa (Tejada-Tovar et al., 2018), oil palm endocarp (Silgado et al., 2014) and litchi husk (Yi et al., 2017). However, most of the research on heavy metal removal by biosorption has been done in batch systems, because they are easy to apply on a laboratory scale but difficult to use on a large scale, particularly when the volume of effluent industry that requires treatment is large (Elabbas et al., 2016). Also, data from batch systems may not be applicable to continuous fixed-bed column operations, where the contact time is not long enough to reach equilibrium (Cherdchoo et al., 2019). Therefore, it is important to determine the practical applicability of a biosorbent in the continuous mode (Bharathi y Ramesh et al., 2013). In large scale process operation, fixed bed column systems are preferred due to their high effectiveness, simplicity of operation, low cost, and ability to scale up from a laboratory process and produce higher quality effluents (Biswas et al., 2020). For the implementation of this technology in a continuous system, adsorption columns are used, with a bed packed with

biomaterials, through which the solution to be treated flows, while the contaminant is retained in the adsorbent material (Ajmani et al., 2020).

In this study, dynamic simulation of the adsorption process was carried out by using Aspen Adsorption V10 program. Few important factors were evaluated systematically while varying in three levels the feed flow (0.75, 1.5 and 3 mL/s), initial concentration (10, 50 and 100 mg/L), bed height (30, 65 and 100 cm) and particle diameter (0.5, 1 and 2 mm) by simulating the estimated mechanism of chromium adsorption in single packed bed column filled with cocoa husk particles by reasonable theoretical assumptions from experimental data such as kinetic model, material balance, isotherm, and heat assumption within the simulation program in order to propose a small-scale adsorption column for single household usage.

2. Methodology

The methodology applied in this study included the following stages: (i) simulation of the adsorption process, (ii) parametric sensitivity analysis. These phases were performed to investigate the factors that affect the dynamic performance of the column. For this, Aspen Adsorption® package was used.

2.1 Data extraction

This study was based on the data collected in the research group and used for a case study for this simulation. The data required for the simulation of the properties of the adsorbent and the adsorption isotherm are presented in Tables 1 and 2, respectively.

Table 1. Physical characteristics of cocoa husk

Parameter	Value
Effective particle size, μm	500
Bulk density, kg/m^3	518

Table 2. Freundlich isotherm parameters

Model	Parameter	Value
Freundlich	$K_F [(\text{mg g}^{-1})(\text{mg L}^{-1})^{-1/n}]$	8.69
	$1/n$	1.53
	R^2	0.9974
	SS	0.5782

The experimental data used as a reference to feed the interface of the simulation program was obtained from the database of the research group on the kinetics of adsorption, and performance of packed bed adsorber for phenol removal using activated carbon from date pits. For the continuous simulation of chromium adsorption on a packed bed of cocoa residue, the below theoretical assumptions were made: (a) Mass/momentum balance: convection without axial dispersion; (b) Pressure Drop Assumption: none; (c) the superficial velocity is constant, thus adsorption from the liquid phase has a negligible effect on the material balance; (d) Kinetic Model: Linear Lumped Resistance; (e) Film Model: Fluid; (f) Isotherm model: Freundlich with independent temperature following the estimated parameter values shown in Table 2; (g) Energy Balance: Isothermal, (h) Molar concentrations are calculated from molar volumes. Ideal mixing is assumed to occur in the liquid phase, so molar volume is a linear function of composition; (i) a lumped mass-transfer rate applies, with a solid-film linear resistance; (j) Mass transfer coefficient is assumed to be constant.

2.2 Mathematical framework

A control volume (V_c) was established, taking into account the cylindrical shape of the adsorption column, with height Δz and a cross-sectional area of the column A . For material balance, a feed flow in which chromium (i) is dissolved was considered, also taking into account the output and accumulation in the control volume defined as shown in Eq(1) (Bahrun et al., 2021).

$$\varepsilon \Delta Z \frac{\delta C_i}{\delta t} = (\mu_0 \varepsilon C_i)_z - (\mu_0 \varepsilon C_i)_{z+\Delta z} - \left(\varepsilon D_{Li} \frac{\delta C_i}{\delta z} \right)_z + \left(\varepsilon D_{Li} \frac{\delta C_i}{\delta z} \right)_{z+\Delta z} - \rho_s \Delta Z \frac{\delta Q_i}{\delta t} \quad (1)$$

When D_{Li} axial dispersion coefficient (m^2/s), ρ_s is the bed superficial density (g/L), μ_0 is the interstitial speed (m/s), z is the bed axial position (m), t is the time (s), C_i is the concentration of chromium in the liquid phase (mg/L), ε is the bed void fraction, and Q_i is the adsorption capacity of cocoa husk (mg/g).

2.3 Parametric studies

The parametric study was carried out to establish the relationship between the different adsorbent particle diameters, feed flow, initial concentration and the different column heights, on the performance of the column by evaluating the bed column rupture curve. packed cocoa shell residue, as shown in Table 3.

Table 3. Physical characteristics of cocoa husk

Parameter	Unit	Range		
		-1	0	1
Feed flow	mL/s	0.75	1.5	3
Initial concentration	mg/L	10	50	100
Bed height	cm	30	65	100
Particle size	mm	0.5	1.0	2.0

From the parametric analysis, optimal values were obtained for the optimal parameters that can obtain the higher C_i/C_o ratio, and the longest penetration time and saturation time. C_i/C_o ratio is the relation between the metal concentrations in the liquid at the outlet and the inlet of the column. Based on the optimization result, the simple design of an adsorption column for chromium removal is determined.

2.4 Sensitivity analysis

The parametric sensitivity analysis was carried out evaluating the effect of the variation of the mass transfer coefficient, bed porosity and isotherm model for each of the selected metals, handling disturbances of one parameter at a time. With the dimensions obtained from the previous analysis, the optimal configuration of each column will be selected. For this, initially, the residual water flow or pollutant concentration curves with respect to time were studied; then, with the previously determined experimental ranges, the effect of the length of the cocoa residual biomass bed was determined (*Theobroma cacao* L.) onto the final concentration of contaminants for different times, as well as the effect of the residual water flow at the inlet of the column. In addition, the effect of the initial concentration of contaminant on the shape of the base curve, and the effect of the diameter of the column on the outlet concentration of the contaminants to be removed were established; from the evaluation of the effect of the mass transfer coefficient, the porosity of the bed, the isotherm model. After that, the operating conditions that maximize the removal of chromium from the residual oils studied on an industrial scale were selected and will be listed to configure an improved case of column operation.

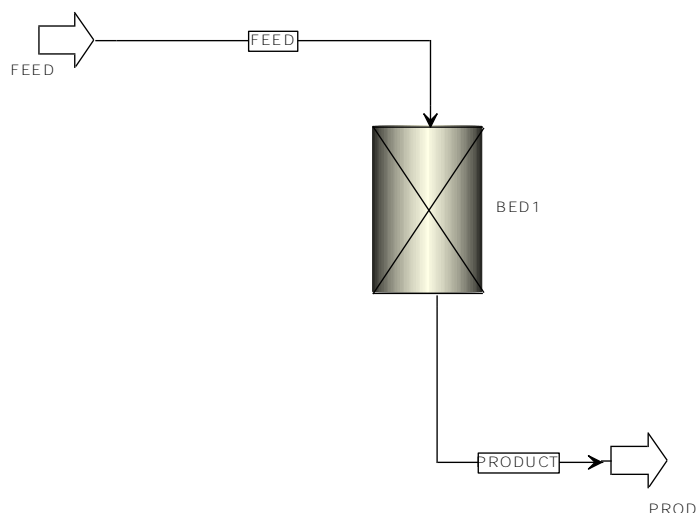


Figure 1. Aspen adsorption flowsheet model.

3. Results and discussion

3.1 Variables affecting the breakthrough curve

The effects of operating parameters as initial concentration, inlet flowrates, bed heights and adsorbent particle size towards the dynamic packed bed column adsorption of Cr (VI) onto cocoa husk were studied and the breakthrough curves of plots of C_t/C_i versus time are presented in Figure 2 (a) to (d).

Table 4. Summary of simulation result of chromium adsorption in column packed with cocoa husk.

Factor	Value	Response		
		Breakthrough time (days)	Breakthrough C_t/C_o ratio	Saturation time (days)
Initial concentration (mg/L)	10	19.54	0.002	294.05
	30	21.48	0.003	235.79
	50	22.50	0.0005	228.04
	100	24.44	0.0032	219.38
Inlet flow (mL/s)	0.75	24.44	0.0032	219.38
	1.5	10.65	0.0032	157.32
	3	3.94	0.032	93.48
Bed height (cm)	30	5.22	0.005	122.05
	65	14.80	0.005	176.31
	100	24.44	0.0032	219.38
Particle size (mm)	0.5	24.44	0.0032	219.38
	1	22.93	0.0005	226.58
	2	20.22	0.0032	230.73

Figure 2a shows comparison of breakthrough curves for various initial concentrations. The simulated breakthrough curve is consistent with a "S" shaped curve, as reported in previous studies (Lin et al., 2017). The inlet Cr (VI) concentrations of 10, 30 50 and 100 mg/L were studied by fixing the values of inlet flowrate, bed height and particle diameter at 7.5×10^{-7} m³/s, 1 m, and 0.5 mm, respectively. From Table 4 and Figure 2, it was observed that when the inlet Cr (VI) concentrations were increased from 10 to 100 mg/L, the breakthrough time increases, from 19.54 to 24.44 days. A high Cr (VI) concentration in the inlet feed causes the system to achieve an early breakthrough. The above, because the increasing in the feed concentration may cause that the adsorption equilibrium will be attained faster due to an increase in the driving force. Thus, more adsorbates being adsorbed because there is more pollutant available and subsequently, shorten the breakthrough time and saturation time of the adsorbent from 294.05 to 219.38 days.

As the bed heights were increased from 30 to 100 cm, the breakthrough time of the column was delayed, from 5.22 to 24.44 days as shown in Figure 2b and summarized in Table 4. A longer bed, provides a larger surface area for a larger mass of Cr (VI) (Haroon et al., 2016), to occupy the active sites available, leading to an increase in the breakthrough time. In addition, the longer the metal ion is in contact with the cocoa husk particles at a longer bed height, therefore, caused a deep transport of Cr (VI) molecules into the adsorbent, thus, results in a higher adsorption of the ions (Fu et al., 2020).

The inlet Cr (VI) flowrates of 0.75, 1.5 and 3.0 mL/s were studied by fixing the values of inlet concentration, bed height and particle size at 100 mg/L, 1 m, and 0.5 mm, respectively. As the inlet flowrates were increased from 0.75 to 3.0 mL/s, the breakthrough curve achieves earlier breakthrough, as shown in Figure 2c. The break point time of the system decreases from 219.38 to 93.48 days as shown in Table 4. This reduction may be due to a chaotic turbulence phenomenon effect to occur along the bed, thus reducing the external mass transfer resistance (Bahrun et al., 2021). The dynamic performance of the cocoa husk in a packed bed column to remove Cr (VI) were studied at 30, 65 and 100 cm, bed heights. The inlet flowrate, inlet concentration and particle size were fixed at 0.75 mL/s, 100 mg/L and 0.5 cm, respectively. Table 6 shows the summary simulation result that was conducted based on different bed height with inlet liquid condition fixed at T = 30 °C, P = 1.0 atm, inlet flow rate of 0.75 mL/s, and initial concentration of 100 mg/L.

The values of inlet flowrate, bed height and inlet concentration were fixed at 0.75 mL/s, 1 m, and 100 mg/L, respectively, in order to evaluate the effect of the particle size. From Table 4 and Figure 2d, it can be said that the effect of the evaluated particle size over the breakthrough curve is negligible. Nevertheless, at lowest particle size, the breakthrough time is longest. One possible reason for this phenomenon is that a lower bed porosity results in higher residence time of the adsorbate in the bed column due to more tortuous path of the adsorbate molecules (Basu et al., 2007).

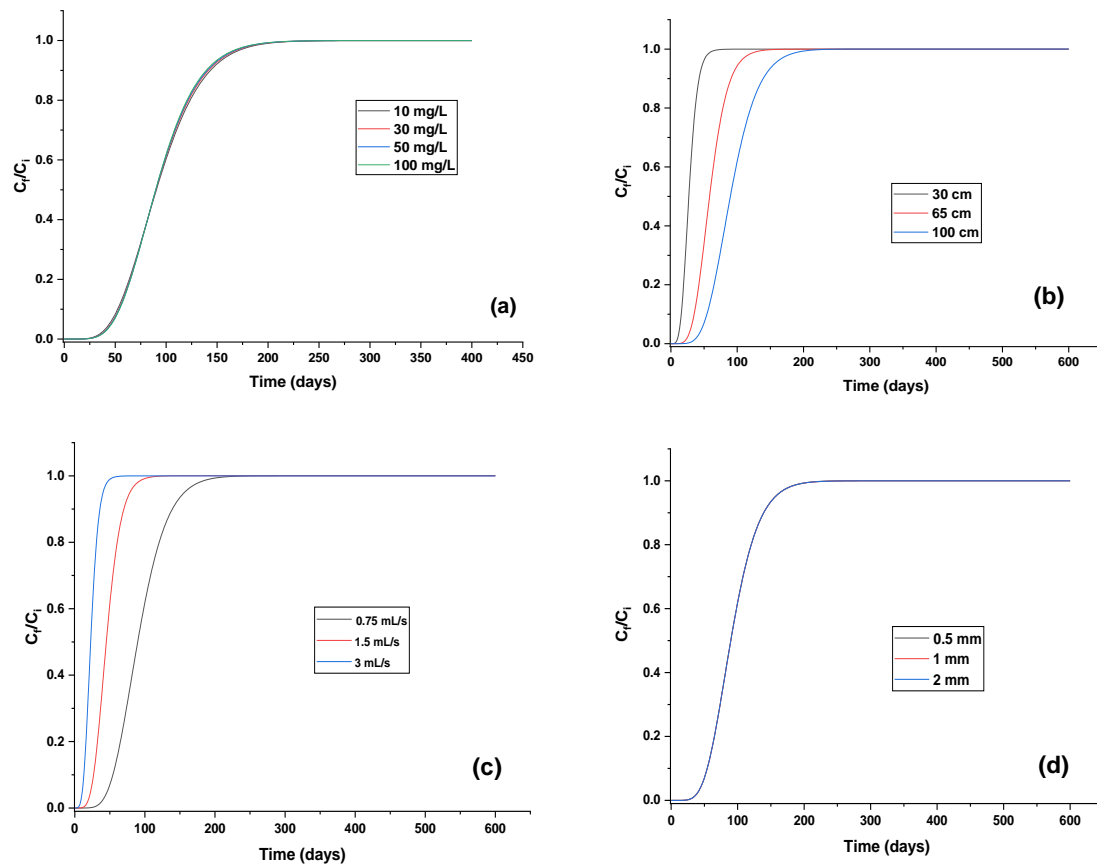


Figure 2. Effect of (a) initial concentration, (b) bed heights, (c) inlet flows, and (d) particle sizes on the breakthrough curves

4. Conclusion

In this study, the simulation of dynamic adsorption of chromium (VI) ions onto cocoa husk in a packed bed column was investigated. Based on the results, some conclusions could be drawn. First, the simulated breakthrough curve is consistent with a “S” shaped curve. The increase of bed height and inlet concentration are directly proportional to the breakthrough time of the system. While the inlet flowrate and particle size of the adsorbent are inversely proportional to the breakthrough time of the system. Bed height and inlet flows effect on the system’s performance is more significant than particle size and initial concentration.

Nomenclature

A – cross-sectional area of the packed bed, m^2
 C_f – final concentration of chromium, mg/L
 C_i – initial concentration of chromium, mg/L
 D_{Li} – axial dispersion coefficient, m^2/s
 t – time, s
 T – temperature, $^{\circ}C$

P – pressure, bar
 Q_i – cocoa husk adsorption capacity, mg/g
 z – bed axial position, m
 ρ_s – bed superficial density, kg/m^3
 μ_0 – interstitial speed, m/s

Acknowledgments

The authors would like to thank the Universidad de Cartagena for the time of the researchers and the laboratory equipment for developing this research.

References

- Afroze S., Sen T. K. 2018. A review on heavy metal ions and dye adsorption from water by agricultural solid waste adsorbents. *Water, Air Soil Pollut.* 229: 225. <https://doi.org/10.1007/s11270-018-3869-z>
- Bahrn M. H. V., Kamin Z., Anisuzzaman, S. M. Bono A. 2021. Assessment of adsorbent for removing lead (Pb) ion in an industrial-scaled packed bed column. *J. Eng. Sci. Technol.* 16: 1213–1231.
- Basu A., Mustafiz S., Islam M. R., Bjorndalen N., Rahaman M. S., Chaalal O. 2007. A comprehensive approach for modeling sorption of lead and cobalt ions through fish scales as an adsorbent. *http://Dx.Doi.Org/10.1080/00986440500193707* 193: 580–605. <https://doi.org/10.1080/00986440500193707>
- Ben Khalifa E., Rzig B., Chakroun R., Nouagui H., Hamrouni B. 2019. Application of response surface methodology for chromium removal by adsorption on low-cost biosorbent. *Chemom. Intell. Lab. Syst.* 189: 18–26. <https://doi.org/10.1016/j.chemolab.2019.03.014>
- Dinh Thi N. 2021. Evaluating the Removal of Hexavalent Chromium (Cr-VI) in Wastewater by Low-Cost Adsorbent Modified from Waste Fly Ash. *Chem. Eng. Trans.* 89: 547–552. <https://doi.org/10.3303/CET2189092>
- Fu W., Ji G., Chen H., Yang S., Yang H., Guo B., Huang Z. 2020. Engineering Anion Resin based Amorphous Molybdenum Sulphide Composite for Treatment of Authentic Acid Mine Drainage. *J. Environ. Chem. Eng.* 8: 104072. <https://doi.org/10.1016/j.jece.2020.104072>
- Gómez-Aguilar D. L., Rodríguez-Miranda, J. P., Esteban-Muñoz, J. A., and Betancur, J. F. 2019. Coffee Pulp: A Sustainable Alternative Removal of Cr (VI) in Wastewaters. *Processes* 7: 403. <https://doi.org/10.3390/pr7070403>
- Haroon H., Ashfaq T., Gardazi S. M. H., Sherazi T. A., Ali M., Rashid N., Bilal M. 2016. Equilibrium kinetic and thermodynamic studies of Cr(VI) adsorption onto a novel adsorbent of Eucalyptus camaldulensis waste: Batch and column reactors. *Korean J. Chem. Eng.* 33: 2898–2907. <https://doi.org/10.1007/s11814-016-0160-0>
- Lam Y. F., Yee L., Chua S. J., Lim S. S., Gan S. 2016. Ecotoxicology and environmental safety insights into the equilibrium, kinetic and thermodynamics of nickel removal by environmental friendly Lansium domesticum peel biosorbent. *Ecotoxicol. Environ. Saf.* 127: 61–70. <https://doi.org/10.1016/j.ecoenv.2016.01.003>
- Lin X., Huang Q., Qi G., Shi S., Xiong L., Huang C., Chen X., Li H., Chen X. 2017. Estimation of fixed-bed column parameters and mathematical modeling of breakthrough behaviors for adsorption of levulinic acid from aqueous solution using SY-01 resin. *Sep. Purif. Technol.* 174: 222–231. <https://doi.org/10.1016/J.SEPPUR.2016.10.016>
- Malise L., Rutto H., Seodigeng T., Sibali L., Ndibewu P. 2020. Adsorption of Lead Ions onto Chemical Activated Carbon Derived From Waste Tire Pyrolysis Char: Equilibrium and Kinetics Studies. *Chem. Eng. Trans.* 82: 421–426. <https://doi.org/10.3303/CET2082071>
- Manjuladevi M., Anitha R., Manonmani S. 2018. Kinetic study on adsorption of Cr (VI), Ni (II), Cd (II) and Pb (II) ions from aqueous solutions using activated carbon prepared from Cucumis melo peel. *Appl. Water Sci.* 8: 36. <https://doi.org/10.1007/s13201-018-0674-1>
- Silgado K. J., Marrugo G. D., Puello J. 2014. Adsorption of Chromium (VI) by Activated Carbon Produced from Oil Palm Endocarp. *Chem. Eng. Trans.* 37: 721–726. <https://doi.org/10.3303/CET1437121>
- Tejada-Tovar C., López-Cantillo K., Vidales-Hernández K., Villabona-Ortiz A., Acevedo-Correa D. 2018. Kinetics and Bioadsorption Equilibrium of Lead and Cadmium in Batch Systems with Cocoa Shell (*Theobroma cacao* L.). *Contemp. Eng. Sci.* 11: 1111–1120. <https://doi.org/10.12988/ces.2018.83100>
- ul Haq A., Saeed M., Anjum S., Bokhari T. H., Usman M., Tubbsum S. 2017. Evaluation of sorption mechanism of Pb (II) and Ni (II) onto pea (*Pisum sativum*) peels. *J. Oleo Sci.* 743: 735–743. <https://doi.org/10.5650/jos.ess17020>
- Wu Y., Fan Y., Zhang M., Ming Z., Yang S., Arkin A. 2016. Functionalized agricultural biomass as a low-cost adsorbent: Utilization of rice straw incorporated with amine groups for the adsorption of Cr (VI) and Ni (II) from single and binary systems. *Biochem. Eng. J.* 105: 27–35. <https://doi.org/http://dx.doi.org/10.1016/j.bej.2015.08.017>
- Yi Y., Lv J., Liu Y., Wu G. 2017. Synthesis and application of modified Litchi peel for removal of hexavalent chromium from aqueous solutions. *J. Mol. Liq.* 225: 28–33. <https://doi.org/10.1016/j.molliq.2016.10.140>